

RETARDING FIELD ENERGY ANALYZERS FOR ION TEMPERATURE MEASUREMENTS IN THE BOUNDARY PLASMAS OF THE TOKAMAK ISTTOK AND TJ-II STELLARATOR

*I.S. Nedzelskiy, C. Silva, H. Fernandes, C. Hidalgo**

*Associação Euratom/IST, Instituto de Plasma e Fusão Nuclear, Instituto Superior Técnico
1049-001 Lisboa, Portugal;*

** Asociacion Euratom/CIEMAT, Av. Complutence, Madrid, Spain*

The retarding field energy analyzer (RFEA) remains the more reliable diagnostic to measure the ion temperature in the boundary plasmas of magnetic fusion devices. A compact, simple design RFEA have been developed for investigations on the tokamak ISTTOK and TJ-II stellarator. More recently a five-channel RFEA has been successfully tested allowing the simultaneous measurement of the ion temperature profile. The conditions of the RFEA operation in poor alignment along magnetic field are considered.

PACS: 52.55.Fa, 52.70.-m, 52.70.Nc

1. INTRODUCTION

One approach to measure an ion temperature in plasma boundary employs a retarding field energy analyzer (RFEA) (see, for example, [1-4]) based on selective rejecting of plasma ions by an electric field. For Maxwellian distribution of the analyzed ions, the collected current as a function of retarding potential, V_r , is given by:

$$I_i(V_r) = I_{0i}, \quad V_r \leq V_{shift}, \quad (1)$$

$$I_i(V_r) = I_{0i} \exp[-q_i(V_r - V_{shift})/kT_i], \quad V_r \geq V_{shift}, \quad (2)$$

where I_{0i} is the ion current collected when none of the ions is repelled by the retarding potential, and V_{shift} is the potential equal to the difference between the plasma potential and the probe ground. Calculations of ion temperature include a least square fitting of the $V_r \geq V_{shift}$ portion of the $I(V_r)$ characteristics to Eq.(2).

One important requirement to the RFEA operation strongly stated in Ref.[4] consists in alignment of the RFEA axis exactly parallel to the local magnetic field direction, so that it is the parallel ion velocity which is measured and not some component of it. The exact fulfillment of this requirement presents definite difficulty when measure T_i profile. However, because the ions with parallel and perpendicular to the magnetic field velocities, moving along helical trajectories, approach the entrance slit with equal probability inside pitch angle cone, one may expect an effective partial compensation of RFEA misalignment and not strongly influencing the results of the measurements.

This work presents RFEAs elaborated for investigations of the boundary plasmas on the tokamak ISTTOK and TJ-II stellarator. RFEA operation in conditions of poor alignment along local magnetic field of the plasma device is considered with reformulation of the alignment requirement in term of RFEA misalignment angle range inside which the obtained results differ within error bars of the measurements.

The paper is organized as follows. The one- and five-channel RFEAs are described in Section 2. The RFEA operation and examples of T_i and T_e measurements on ISTTOK with aligned RFEA are shortly presented in Section 3. Section 4 considers dependence of the RFEA characteristics on alignment along magnetic field. Summary is done in Section 5.

2. RFEA DESCRIPTION

Fig.1 shows the picture and schematic of one-channel RFEA [5]. It includes an input stainless still slit ($3 \times 0.1 \text{ mm}^2$), three fine Nickel grids and copper collector plate, all separated by MICA insulators (1 mm of distance between grids). The grid and collector stack are assembled inside boron nitride housing. The dimensions of one-channel RFEA are $14 \times 14 \times 23 \text{ mm}$.

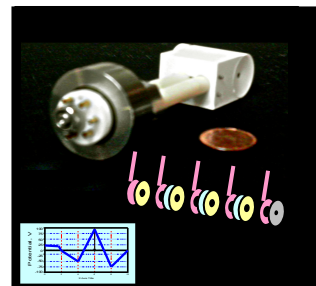


Fig.1. Picture and schematic of one-channel RFEA

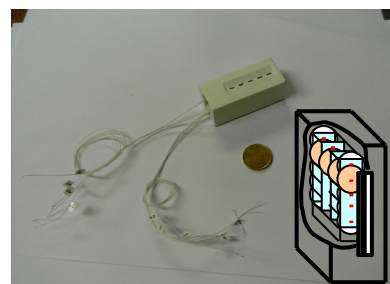


Fig.2. Picture and schematic of five-channel RFEA

Recently, a five-channel RFEA to measure simultaneously the profile of T_i has been developed, assembled and tested. Design of five-channel RFEA shown in Fig.2 presents just a compilation of the one-channel RFEA with common grids in all channels and multiplied number of slits and collectors. Usage of common grids sufficiently simplifies RFEA powering and operation. The dimensions of five-channel RFEA are $20 \times 24 \times 55$ mm, and distance between slits is 7 mm.

A standard biasing configuration is shown in the inset of Fig.1. An operational amplifier is employed for triangle shape biasing of the retarding grid. The current collected by the RFEA is measured across a resistor with isolation amplifier and acquired by ISTTOK data acquisition system (up to 2 MHz sampling rate).

3. RFEA OPERATION

RFEAs operation has been tested in plasma of ISTTOK ($R = 0.45$ m, $a_{lim} = 0.078$ m, $a_{vessel} = 0.1$ m, $B = 0.5$ T) with $\langle n_e \rangle = (2 \dots 3.5) \times 10^{18} \text{ m}^{-3}$, $T_e(0) \sim 150$ eV, $I_p = (2.5 \dots 5)$ kA, $\tau_{shot} = 20$ ms. RFEAs are installed in a horizontal diagnostic port of ISTTOK and can be shot-by-shot moved radially and rotated ($\pm 30^\circ$) by vacuum manipulator.

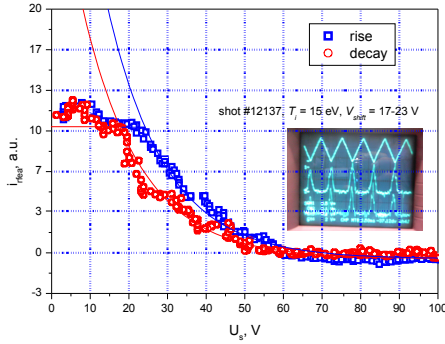
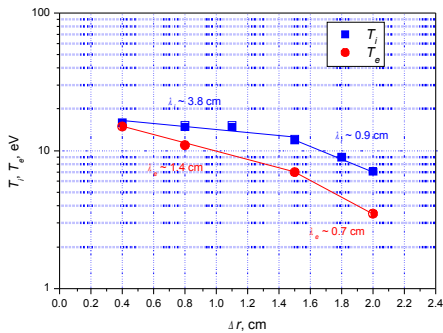


Fig.3. Typical ion mode signals from two RFEA channels (inset) and signal fitting by function of Eq. (2)

An inset in Fig.3 shows typical ion mode signals from two channels of five-channel RFEA aligned along magnetic field of ISTTOK. An example of ion



characteristic, as well as the respective fitting, is presented in Fig.3.

Fig.4. Profiles of T_i and T_e measured by RFEA on ISTTOK

Fig.4 presents the profiles of T_i and T_e at flat top of the discharge measured with RFEA on ISTTOK (in electron

mode the polarity of the potentials applied to the RFEA grids is reversed).

4. DEPENDENCE ON ALIGNMENT ALONG MAGNETIC FIELD

In experiments on TJ-II, the RFEA expects fast reciprocation across magnetic field surfaces, therefore operating at slightly different angles (estimated as up to 6° range) between analyzer axis and magnetic field line. Poor alignment conditions have been investigated with one-channel RFEA rotated relative magnetic field line of ISTTOK plasma.

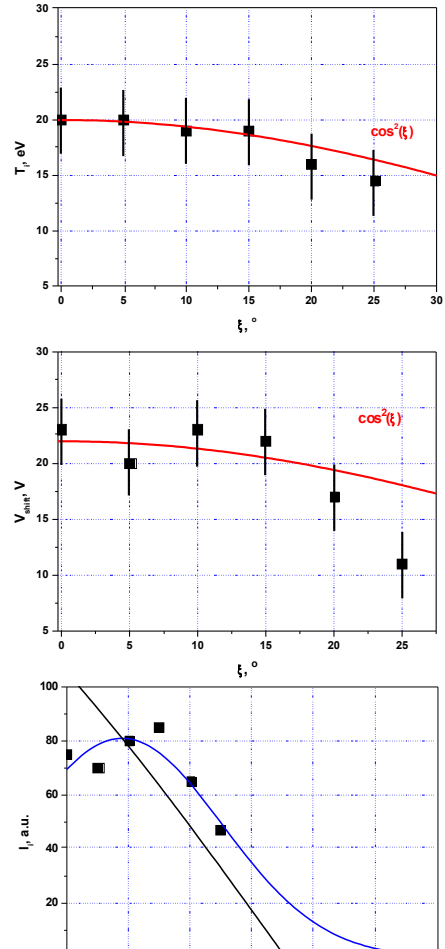


Fig.5. Results of T_i (top), V_{shift} (middle) and unbiased collected current (bottom) for different ξ

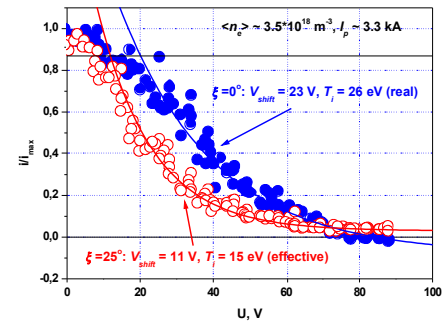


Fig.6. Example of the normalized retarding curves at $\xi \sim 0^\circ$ and $\xi \sim 25^\circ$

Fig. 5 present the example of obtained results of T_i (top), V_{shift} (middle) and unbiased collected current (bottom) measured for different angles, ξ , in the range of

$\xi = (0 \dots 25^\circ)$ for plasma with $\langle n_e \rangle = 2.5 \times 10^{18} \text{ m}^{-3}$ and $I_p = 2.5 \text{ kA}$. The error bars are mainly determined by noise of the signal. Fig. 6 shows the example of the normalized experimental retarding curves at $\xi = 0^\circ$ and extreme $\xi = 25^\circ$ demonstrating clear modifications of measured values of T_i and V_{shift} . Contrary, the unchanged inside error bars values of both T_i and V_{shift} in the angle range of $\xi \sim \pm 10^\circ$ can be identified. Fitting the unbiased collected current data by Gaussian function gives HWHM $\sim \pm 20^\circ$ and peaks at $\xi_0 \sim 9^\circ$ for $I_p = 2.5 \text{ kA}$ and at $\xi_0 \sim 7.7^\circ$ for $I_p = 3.5 \text{ kA}$, indicating (expected) correlation with plasma current.

Qualitatively, the observed results can be partially understandable from idealized non-magnetized 2D model for the parallel uniformly distributed across RFEA slit particle flow with shifted Maxwellian distribution ($E_b = V_{shift}$ and $\Delta E_b = T_i$). Taking into account that to cut the particle entering into analyzer at some angle ξ relative to the analyzer axis, the potential applied to the retarding grid is lower on the value of $\Delta V_r = \Delta E_{||} \sin^2 \xi$, Eq.(1) and Eq.(2) can be rewritten as:

$$I_i(V_r) = K_M I_{0i}, \quad V_r \leq V_{shift} \cos^2 \xi, \quad (3)$$

$$I_{i(i)}(V_r) = K_M I_{0i} \exp[-q_i(V_r - V_{shift} \cos^2 \xi)/kT_i \cos^2 \xi], \quad V_r > V_{shift} \cos^2 \xi, \quad (4)$$

where $K_M = \cos^2 \xi [1 - (l/a) \tan \xi]$ is the RFEA transmission factor in optical approximation (l is the analyzer length from input slit to collector, and a is the analyzer aperture after input slit), and Eq.(4) is derived from Eq.(2) by rescaling V_r as $V_r / \cos^2 \xi$.

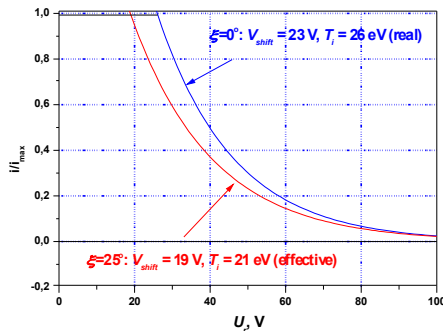


Fig. 7. Normalized retarding curves for two entering angles of 0° and 25° calculated with Eq. 4

Fig. 7 (top) presents normalized retarding curves, I_i/I_{max} , calculated for two entering angles of $\xi = 0^\circ$ and $\xi = 25^\circ$, showing similarity with experimental results (for comparison, $\cos^2 \xi$ curves are drawn in experimental data of Fig. 5 also). Shown in Fig. 5 (bottom) the calculated dependence of unbiased current (or K_M for $l = 4 \text{ mm}$, $a = 2 \text{ mm}$) on entrance angle predicts fast decay in contradiction with the experimental results. It means (and not surprisingly) violence of linear optical transmission approximation for magnetized particle flux. Notice, however, quite good agreement of experimental $\frac{1}{2}(\text{FWHM}) \sim 20^\circ$ with calculated complete cutting at $\xi_{cut} = \text{atan}(a/l) = 26.6^\circ$.

5. SUMMARY

A compact, simple design one- and five-channels RFEAs have been developed for investigations of boundary plasmas on the tokamak ISTTOK and TJ-II stellarator. The ion and electron temperature profiles have been successfully measured on ISTTOK.

The investigations of dependence of the RFEA characteristics on alignment along magnetic field of ISTTOK show the unchanged inside the error bars results for both T_i and V_{shift} in the angle range of $\xi \sim \pm 10^\circ$. Presumable, the ion pitch angle could be candidate for explanation of the observed properties.

ACKNOWLEDGEMENTS

This work has been carried out in the frame of the Contract of Association between the European Atomic Energy Community and Instituto Superior Técnico (IST) and of the Contract of Associated Laboratory between Fundação para a Ciência e Tecnologia (FCT) and IST. The content of the publication is the sole responsibility of the authors and it does not necessarily represent the views of the Commission of the European Union or FCT or their services

REFERENCES

1. G.F. Matthews// *J. Phys. D*, 1984, v. 17, p. 2243.
2. A.S. Wan, T.F. Yang, B. Lipschultz, B. LaBombard// *Rev. Sci. Instrum.* 1986, v. 57, p. 1542.
3. R. A. Pitts// *Phys. Fluids B*. 1991, v. 3, p. 2871.
4. G.F. Matthews, R.A. Pitts, G.M. McCracken, P.C. Stangeby// *Nucl. Fusion*. 1991, v. 31, p. 1495.
5. I.S. Nedzelskiy et al// *Rev. Sci. Instrum.* 2006, v. 77, p. 10E729.

Article received 22.09.08

АНАЛИЗАТОР ЭНЕРГИИ С ЗАДЕРЖИВАЮЩИМ ПОТЕНЦИАЛОМ ДЛЯ ИЗМЕРЕНИЯ ТЕМПЕРАТУРЫ ИОНОВ НА ГРАНИЦЕ ПЛАЗМЫ В ТОКАМАКЕ ISTTOK И СТЕЛЛАРАТОРЕ TJ-II

I.S. Nedzelskiy, C. Silva, H. Fernandes, C. Hidalgo

Анализатор энергии с задерживающим потенциалом (АЭЗП) остается наиболее надежным диагностическим устройством для измерения температуры ионов вблизи границы плазмы термоядерных установок с магнитным удержанием. Компактное простое устройство АЭЗП разработано для исследований на токамаке ISTTOK и стеллараторе TJ-II. Сравнительно недавно пятиканальный АЭЗП был успешно испытан и позволяет осуществлять синхронные измерения профиля температуры ионов. Определены условия работы АЭЗП при плохой ориентации его вдоль магнитного поля.

АНАЛІЗАТОР ЕНЕРГІЇ З ЗАТРИМУЮЧИМ ПОТЕНЦІАЛОМ ДЛЯ ВИМІРУ ТЕМПЕРАТУРИ ІОНІВ НА ГРАНИЦІ ПЛАЗМИ В ТОКАМАЦІ ISTTOK І СТЕЛЛАРАТОРІ TJ-II

I.S. Nedzelskiy, C. Silva, H. Fernandes, C. Hidalgo

Аналізатор енергії з затримуючим потенціалом (АЕЗП) залишається найбільш надійним діагностичним пристроєм для виміру температури іонів поблизу границі плазми термоядерних установок з магнітним утриманням. Компактний простий пристрій АЕЗП розроблено для досліджень на токамаці ISTTOK і стеллараторі TJ-II. Порівняно недавно п'ятиканальний АЕЗП був успішно випробуваний і дозволяє здійснювати синхронні виміри профілю температури іонів. Визначено умови роботи АЕЗП при поганий орієнтації його уздовж магнітного поля.